Effects of temperature and concentration on mechanism and kinetics of thermally induced deposition from coffee extracts

Marek Kroslak[1,3], Massimo Morbidelli[1], Jan Sefcik[2*]

[1]Institut für Chemie- und Bioinginieurwissenschaften, ETH Zurich, Zurich, Switzerland
[2]Department of Chemical and Process Engineering, University of Strathclyde, Glasgow, UK
[3]Present address: SEP Salt & Evaporation Plants Ltd., Winterthur, Switzerland

Corresponding author: Jan Sefcik, E-mail: jan.sefcik@strath.ac.uk, Address: University of Strathclyde, 75 Montrose Street, Glasgow, G1 1XJ, UK

Production of soluble (instant) coffee powders typically involves extraction of roasted coffee by water followed by evaporation in order to concentrate extracts before spray or freeze drying to produce dry coffee powder. In the course of evaporation, deposition of dissolved material from coffee extracts is a major cause of fouling at heat exchange surfaces of evaporators. Therefore in order to improve design and optimization of evaporation processes of coffee extracts, a better understanding of deposition mechanism and kinetics is needed. We used Optical Waveguide Lightmode Spectroscopy (OWLS) to monitor the initial formation of nanometer scale deposits on surfaces exposed to coffee extracts. OWLS measurements were complemented by light scattering from extract solutions, gravimetry of macroscopic deposits and scanning electron microscopy imaging of deposited layers. Primary molecular-scale layers of about 1 mg/m^2 were rapidly formed in the first stage of deposition even at ambient temperature, followed by the secondary deposition with kinetics strongly dependent on temperature. Secondary deposition rates were low and largely independent of the extract concentration at ambient temperature, but became strongly dependent on extract concentration at elevated temperatures. In particular, activation energies for deposition between 25 and 70°C were much higher for the original extract (13.3% w/w solids) than for diluted extracts (up to 1.3% w/w solids). Furthermore, heating of the original extracts above 60°C resulted in rapid aggregation of suspended macromolecules into large clusters, while only gradual aggregation was observed in diluted extracts.

Keywords: coffee extracts; deposition; aggregation; fouling; evaporation; heat exchange

Introduction

Deposition and fouling play an important role in various industrial and biomedical applications, such as filtration, heat exchange, evaporation, deposition in blood vessels, implant biocompatibility and others. There are instances where deposition is desired, as long as it can be controlled, but others where it is not. Typical examples are in food processing industries, where various liquids (solutions or dispersion) are treated in falling film evaporators in order to produce more concentrated solutions. Extensive fouling of evaporator surfaces can occur over a period of hours to days, depending on properties of a particular system. Fouling leads to build-up of a thick layer deposited on the evaporator surface, which causes a gradual decrease in the efficiency of the heat transfer and the eventual interruption of the production process in order to proceed to surface cleaning.

Various characterization methods have been used to study fouling kinetics. Macroscopic deposits can be conveniently studied using gravimetry, which has the advantage of relative simplicity and direct data interpretation. Quartz crystal microbalance has been used to study protein adsorption and it provides useful quantitative information related to mass and viscoelastic properties of deposited material (Höök et al., 2002). Another useful technique widely used in fouling studies is optical microscopy, providing visual characterization of deposited layers down to the micrometer scale. Scanning electron microscopy or atomic force microscopy can provide details in the nanometer range, but they typically require sample manipulations, which may lead to significant changes with respect to its original morphology. This especially concerns biological systems, which are often sensitive to changes in the environment.

On the other hand, spectroscopic characterization methods can provide molecular level insight into the mechanisms governing the deposition process, especially at its early stages. Surface spectroscopic techniques, such as Optical Waveguide Lightmode Spectroscopy (OWLS), have the advantage of non-destructive, in situ monitoring of solid-liquid interfaces and provide a useful tool to study adsorption and deposition at solid-liquid interfaces. A limitation of this and similar reflectance-based techniques (e.g., ellipsometry, reflectometry) is that there is a limited extent of the deposit thickness that can be measured, typically not exceeding few tens of nanometers. OWLS is especially suitable to study interfaces interacting with dense and/or dark suspensions,

since this waveguide-based method does not require the reflecting laser beam to pass through the suspension.

The extracts obtained from ground roasted coffee beans are darkly colored mixtures containing proteins, polysaccharides and organic acids in both soluble and insoluble (colloidal) form suspended in an aqueous matrix. We note that there is a significant amount of lipids in (roasted) coffee beans, but lipids are poorly soluble in water and their concentration in coffee extracts is therefore very low. We are not aware of any previous studies on deposition from coffee extracts or similar systems. Most of previous studies about surface fouling refer to the deposition of proteins, mostly of animal origin. When protein solutions come into contact with an interface a spontaneous deposition is typically observed. Published studies have been mostly focused on protein-surface interactions, mainly at ambient temperature. Protein deposition is affected by pH, electrolyte concentration and temperature, which may specifically affect the protein functional groups or change its geometrical arrangement. Polysaccharides, which represent a significant component of the coffee extracts, tend to copolymerize with proteins at elevated temperatures (Maillard reaction), and the resulting copolymers are also expected to be subject to fouling.

Considering interphase interactions of deposited entities with solid surfaces, we can divide the deposition processes into two main groups:

i) The first group involves monolayer systems, where the main driving force for the deposition is due to the interaction potential difference between a bulk solution and a solid surface. Electrostatic double layer repulsion prevents charged polymer colloids from aggregating to each other, resulting in a stable deposited monolayer on the solid surface, which is made resistant against further deposition by the same electrostatic repulsive forces which keep suspended colloids stable in the bulk solution.

ii) The second group involves multilayer systems, where the repulsive interactions between the primary deposited layer and the bulk solution entities are reduced, so that subsequent deposition on the top of the primary layer can proceed. Multilayer growth can be achieved by altering the bulk solution composition, mainly through changes of pH and/or electrolyte concentration or, as in the system studied here, by increasing the temperature. Typically, fouling phenomena occur through the multilayer deposition. In this case the deposition is driven by interactions of previously deposited entities with those in the bulk, similar to aggregation in the bulk solution itself, so that fouling becomes independent from surface properties of the original substrate after the first few layers are deposited.

Multilayer film deposition at ambient temperature was studied by Picart et al. and Lavalle et al. (Picart et al., 2001; Lavalle et al., 2004), where well defined polyelectrolyte multilayers and multilayer polyelectrolyte/protein films were investigated by OWLS and scanning angle reflectometry. It was shown that OWLS was able to monitor the deposition process from the initial deposited layer up to a thickness of more than 40 nm, while reflectometry could be used only after a few nanometers have been deposited up to about the same maximum thickness. This study of polyelectrolyte multilayer growth pointed out the important role of solution pH and charge distribution inside the film on the layer buildup mechanism.

Studies of Griesser et al. (Griesser et al., 2002) on the deposition of complex protein mixtures (differing in the isoelectric point) for different bulk solution electrolyte concentrations on variously grafted polysaccharide layers and polymer coatings showed that coatings with substantial surface charge can be resistant to protein adsorption of the same charge, although they cannot be considered as a universal protein-resistant surface for all protein mixtures.

The effect of temperature, particularly at elevated temperature, on the deposition process has been rarely investigated. As reported in the review by Nakanishi et al. (Nakanishi et al., 2001), this may be in part related to the associated experimental difficulties. The most commonly temperature driven fouling system studied in the literature is milk (Changani et al., 1997; Jong, 1997; Visser & Jeurnink, 1997; Anema, 2000). This is a complex mixture of proteins, fats, carbohydrates, minerals and enzymes. There are two major components playing a role in milk fouling. Deposits formed between 60°C and 100°C are predominantly proteinaceous (with β-lactoglobulin as the dominant protein), while deposits formed above 100°C are rich in minerals. Thermal properties and aggregation and deposition behavior of proteins are in general strongly dependent on pH and on the presence of other components, such as calcium ions, lactose or casein. Upon heating at neutral pH, the proteins initially unfold and expose their inner hydrophobic cores and free thiol groups, which initiates their spontaneous aggregation and can also lead to their deposition on surfaces (Kroslak et al., 2007; Vogtt et al., 2011; Grancic et al., 2012). At ambient temperature β-lactoglobulin forms monolayer due to its interaction with the bare surface, which is the typical behavior observed for various proteins (Relkin, 1996; Van Tassel, 2003; Voros, 2004; Sava et al., 2005).

The main scope of this work was to investigate the mechanism and kinetics of surface deposition from coffee extract induced by an increased temperature. Using the temperature control setup developed for the OWLS instrument allowed us to obtain unique insights into the

deposition process in these systems. A better qualitative and quantitative understanding of the deposition process should provide a rational basis for possible process modifications leading to decreased fouling, thus improving the heat transfer in evaporators used for the production of concentrated extracts.

In the following we investigate the primary layer formation on several different surfaces at ambient temperature and at various pH and electrolyte concentrations. Next, we investigate the secondary deposition driven by temperature on the primary layers previously deposited on a silica surface. The structure of deposited layers is also analyzed using scanning electron microscopy while the macroscopic deposition kinetics at longer times is measured by gravimetry. Light scattering is used to monitor the corresponding aggregation processes in the bulk suspension for variously diluted extracts at elevated temperatures.

Optical Waveguide Lightmode Spectroscopy

Optical waveguide lightmode spectroscopy is based on measurements of changes of the effective refractive index of an optical waveguide when a thin film forms at the waveguide surface. The presence of the thin film changes the evanescent electromagnetic field in a close vicinity of the waveguide surface and it influences the light reflection from the waveguide surface. This results in a shift of the incidence angle of a light beam leading to a lightmode guided along the waveguide. By measuring the incidence angle α corresponding to the resonance maximum of the light incoupled in the waveguide it is possible to determine an effective refractive index N of the light propagating along the waveguide and from that the thin film (deposited) mass per surface area (please see further details in Supplementary Information).

Experimental

Materials

The dry solid content of the coffee extract (provided by Nestlé Product Technology Centre Orbe, Switzerland) considered in this work is 13.3 wt% and the pH is 5.0. The dry mass of the suspension is constituted of 7.4% proteins, 35% carbohydrates, 3.2% minerals and 54.4% other organic molecules like melanoidines, organic acids and ash. At the natural pH of the coffee extract (pH 5) most of the proteins are negatively charged (36%), 1.2% are positively charged, 30% are polar uncharged (mainly aliphatic), 23% are aromatic and the rest is not determined. The

148 sediments constitute 2% of the overall dry content. All solutions were prepared with ultra pure
149 water (Millipore, 18MΩ) degassed under vacuum before use in order to reduce bubble formation
150 in the spectroscopy cell.
151 Silica-Titania planar waveguides (OW 2400) were purchased from Microvacuum Ltd.
152 (Budapest, Hungary). They consist of a 1-mm-thick AF45 glass substrate and a 180-nm thick
153 $Si_{0.75}Ti_{0.25}O_2$ waveguiding surface layer, with dimensions of 1.2x0.8x0.1cm. The isoelectric point
154 (IEP) of silica is 3.0 and of titania around 5.5 (Kosmulski, 2001). The waveguide layer has an
155 approximate thickness of t_F~180nm and a refractive index of n_F~1.76. Five different surfaces
156 have been used in this study to investigate the ambient temperature deposition process. These
157 include the negatively charged silica and niobia surfaces, the positively charged alumina surface,
158 and the hydrophobic polystyrene (PS) and poly(ethylene glycol)-3.5-poly(L-lysine) (PEG-3.5-
159 PLL) surfaces. At elevated temperature only the silica modified surface has been used.
160 All the surfaces mentioned above have been obtained through a suitable coating procedure,
161 covering the original waveguide film with layers 10-15 nm thick. The silica and alumina coated
162 waveguides were purchased from Microvacuum Ltd. (Budapest, Hungary). The IEP of alumina is
163 8 (Kosmulski, 2001). The niobia coated waveguides were sputter coated on the original
164 waveguide, using reactive magnetron sputtering (PSI, Villigen, Switzerland). The IEP of niobia is
165 4.3. Before each deposition experiment, all oxide surfaces were activated in NaOH solution at pH
166 11 for 3 hours. Afterwards, the waveguides were rinsed with Millipore water and dried with
167 nitrogen. This procedure activates the hydroxyl groups on the accessible surface.
168 A polystyrene (PS) layer approximately 15 nm thick was coated on the silanized original
169 waveguide using 1% polystyrene dissolved in toluene at rotation speed 3000 rpm for 1 minute
170 (Extrand, 1994; Schubert, 1997). PS used in this study was PS Standard 30'000 from Sigma-
171 Aldrich (Product Number 81408) with M_p=32500, M_n=31000, M_w=32000, M_w/M_n=1.02.
172 Silanization by hexamethyldisilazane, from Fluka, (Lot. No. 427155/1 44601) was used to make
173 the originally hydrophilic oxide surface hydrophobic (Huang, 2002). PEG-3.5-(PLL), a
174 polycationic co-polymer (grafting ratio of 3.5; Huang, 2002), positively charged at neutral pH
175 (Huang, 2002), was spontaneously adsorbed on the negatively charged original surface from
176 aqueous solution. PEG-3.5-(PLL) modified waveguides were obtained from the Laboratory of
177 Surface Science and Technology, Department of Materials, ETH Zurich.
178 Prior to the SLS measurements the coffee extract was filtered with a 0.8 μm filter (Millipore) in
179 order to remove bigger aggregates from the coffee extract. This does not change significantly the

overall dried mass of the filtrate compared to the original extract. The removal of these particles is needed to reduce skewing of the measurements caused by big aggregates.

OWLS

Deposition experiments were performed in OWLS apparatus type OWLS 110 made by Micro Vacuum Ltd, Budapest, Hungary with an integrated temperature control unit. The waveguide is placed in a measuring cell, which is a channel 8mm long with rectangular cross section (0.8mm high and 2 mm wide) with a volume of 12.8μl, with entrance and exit ports to allow for continuous flow through. All delivery tubes and the measuring cell are made of PTFE. The flow through operation mode has been selected in order to guarantee exposure to a fresh extract with constant composition over time. The waveguide parameters n_f and t_f are measured through a preliminary set of experiments where water is flushed through the deposition cell at ambient temperature.

In the deposition experiments at ambient temperature the waveguide surface was exposed to the coffee extract for at least one hour leading to completion of the primary deposited layer on the bare surface. The flow rate is held constant at 1ml.min^{-1} by the programmable syringe pump Vit-Fit (Lambda, Czech Republic). After deposition, the sample is washed with water for at least 1 hour at ambient temperature. This was found sufficient to wash out all the electrolytes adsorbed on the deposition process.For the runs at higher temperatures, a specific experimental procedure has been developed which is described in detail in Supplementary Information. After each deposition experiment the waveguide was cleaned by a short exposure to a strong oxidizing agent (3 seconds in chromic acid), followed by water rinsing. After the cleaning procedure, the position of the resonance spectra was checked and compared with the initially measured one to check that no waveguide damage occurred during cleaning.

Gravimetry

Gravimetry measurements were used as complementary experiments for OWLS measurements. While the OWLS was used in this work to track deposition for surface coverages up to 30 mg.m^{-2}, in order to study the deposition at longer times, when thicker deposits are obtained, we used gravimetry, the lower detection limit of which for the given experimental system is about 50 mg.m^{-2}. Gravimetry is probably the most conventional method to study macroscopic deposition. It is based on weighing the difference between adsorbent weight before and after the adsorption process, and therefore its sensitivity is limited by the accuracy of the weighting procedure. The silica plate was placed into a gravimetry cell, constituted by a channel 180 mm long, with

rectangular cross-section 0.5 mm high and 18 mm wide. All delivery tubes were made of stainless steel and the gravimetry cell was made of alumina. The channel geometry has been selected so that we can use the hydrodynamic model for laminar flow between two infinite parallel plates to calculate the hydrodynamic regime inside the channel. Using this model we can determine the flow rate to be fed to the channel so that the velocity gradient at the surface of the waveguide is equal to that in the OWLS cell. The calculated velocity gradient in the OWLS cell is about 500 s^{-1}, which corresponds to a volume flow rate in the channel of 32ml.min^{-1}. A peristaltic pump was used to deliver the extract preheated to the desired temperature shortly before entering the measurement cell. The entire gravimetry cell was held at constant temperature. Washing with pure water was performed for one hour after the cooling step as in the OWLS experiments.

Light scattering

Light scattering experiments were performed on coffee extract in order to compare the aggregation in the liquid bulk with the surface deposition. All measurements have been taken with a small angle light scattering instrument (Mastersizer 2000 by Malvern) after preliminary filtration with 0.8μm filter. The original extract was heated and kept for one hour at constant temperature in the range 25-80ºC so as to undergo Brownian aggregation. Samples were withdrawn at fixed times and quickly diluted 200 times with pure water in order to stop aggregation and avoid multiple scattering in the light scattering measurements. Alternatively, the extract was immediately diluted and then heated at the desired temperature so as to monitor directly in-situ the aggregation process by light scattering without any sampling procedure.

Results and discussion

Estimation of OWLS parameters

In order to evaluate the deposited mass from the measured *N(TE)* we need to supply optical parameters which correspond to the conditions inside the deposition cell. The refractive indices n_S and n_C, for the waveguide support and the cover liquid, respectively have been taken from the literature or measured independently at various temperatures and are summarized in **Table 1**. The waveguide thickness t_F and refractive index n_F may vary slightly depending on the measurement conditions and therefore have been evaluated before each experiment.

Let us now consider the evolution of the derivative of the dielectric constant with respect to the mass concentration of deposit $\mathrm{d}c/\mathrm{d}\varepsilon$ (see Supplementary Information for further details). For this the refractive indices of variously diluted coffee extracts were measured by refractometer at wavelength 632.8nm for four different temperatures (20, 25, 40, 60℃). The measured values are provided in **Table 1** where x_E represents the weight concentration of solid content in coffee extract suspension. Since the relative dielectric constant can be computed from the refractive indices in the table as $\varepsilon = \mathrm{n}_\mathrm{C}^2$, the derivative $\mathrm{d}c/\mathrm{d}\varepsilon$ (where c=x_E) can be readily obtained. This procedure has been repeated at the four considered temperatures and obtained values are fitted by following expression, where T is given in ºC:

$$\left(\frac{\mathrm{d}c}{\mathrm{d}\varepsilon}\right)_\mathrm{T} = -3.47\cdot10^{-6}\mathrm{T}^2 + 4.028\cdot10^{-3}\mathrm{T} + 1.642 \quad [\mathrm{g/cm^3}] \tag{1}$$

As can be seen for this particular case, the term $\mathrm{d}c/\mathrm{d}\varepsilon$ changes just very little within measured temperature range 20-60℃ (i.e. a temperature change of 40℃ leads to an increase of 3%). Here we can notice that the value determined experimentally at ambient temperature for the coffee extract (1.74 g.cm^{-3}) is similar to the value conventionally used to determine the deposited mass from various biomolecular systems (~1.89 g.cm^{-3}) (Defeijter, Benjamins & Veer, 1978).

Deposition at ambient temperature

A typical result of the OWLS measurement is shown in **Figure 1** in terms of mass deposited during a primary exposure of two waveguides, the silica and the polystyrene coated ones, to the coffee extract (solid concentration 13.3 wt%). After equilibration with pure water the extract was pumped at constant flow rate through the measuring cell, and at the end of the deposition process the flow was switched back to pure water and the washing process started. These two times are indicated by arrows in the figure. Typical deposition coverage was about 1 mg.m^{-2} after washing with pure water for one hour at ambient temperature.

It can be seen that in the case of the hydrophobic polystyrene coated waveguide the deposited mass increased almost instantaneously to about 2 mg.m^{-2}, and then under very slow growth, which in the following we refer to as the secondary growth. During washing there was a rapid decrease of the deposited mass to about 1 mg.m^{-2}, followed by a period of time where the mass decrease was so slow that we can consider the deposit as stable in time. When the silica surface was exposed to the extract, the deposited mass was growing rapidly for a longer time, i.e. about half an hour, followed again by a steady but very slow increase corresponding to the so-called secondary growth. Also in this case washing starts very fast and then slows down considerably,

leading to a stable deposit. The mass measured at this point represents the amount of material irreversibly deposited on the surface, since the waveguide is at the same conditions as at the beginning of the experiment (in contact with pure water at ambient temperature). And this will be referred to in the following as irreversible primary layer.

It is worth noting that while the response of the neutral polystyrene surface is almost instantaneous, the one of the charged silica surface is slower and more pronounced. This is due to the fact that in the second case not only the extract material, but also all the various electrolytes present in the solution are adsorbed or deposited on the surface. These species are however removed during washing, so that it can be observed that the irreversibly deposited amount is very close to that obtained for polystyrene. This can be confirmed by the data reported by Nellen et al. (Nellen et al., 1992) for simple electrolyte solutions, which indicate typical saturation times of about 40 min.

The sensitivity of the silica waveguide to electrolytes is well known and the usual way to eliminate it is to use a background medium with the same electrolyte composition as the covering liquid under examination. Since the coffee extract used here was a complex buffering mixture, it was not possible to prepare a matching background medium. Therefore, in addition to the deposition of the extract components, we need to take into account the partitioning equilibrium between the solution and the solid surface. The closer the solution pH is to the isoelectric point of a given surface, the less significant the adsorption of electrolytes is (Sefcik et al., 2002). When the silica surface is exposed to an electrolyte solution at pH=3, which corresponds to its isoelectric point, there is no charging response from the waveguide surface, similarly to the case of neutral polystyrene surface.

In **Figure 2** we show the results of deposition measurements for multiple subsequent exposures of a silica coated waveguide to the coffee extract. The first exposure leads to the formation of an irreversible primary layer of about 1.2 $mg.m^{-2}$ as shown in **Figure 1**. The second and third exposures exhibit a very similar behavior. It is worth noticing that for all three subsequent exposures, although the secondary growth region was extended over different times, the final irreversible deposit was substantially the same. This indicates that the material deposited during secondary growth is weakly bounded to the surface and is easily removed by washing with water.

The values of the irreversibly deposited mass obtained after the primary exposure to the extract on various surfaces are summarized in **Table 2**. Note that the obtained values are in the same range as those observed for pure proteinaceous solutions deposited on silica surfaces (Nakanishi

et al., 2001). Silica and niobia surfaces (isoelectric point at pH 3 and 4, respectively) are negatively charged in contact with the extract at its native pH 5 and exhibit the same thickness of the deposit. A comparable deposited mass was observed on polystyrene (neutral hydrophobic surface) after 15min of exposure, thus confirming that the irreversible primary layer builds up almost completely after quite a short time. The amounts deposited on PEG-3.5-PLL (positively charged at pH 5 since it contains sterically isolated amine groups) and alumina surfaces (positively charged) were smaller than those in the previous cases. It is remarkable that the extract dilution does not lead to any substantial difference in the deposited amount of primary layer, as shown by data in **Table 2** for silica coated waveguide.

These data confirm the result reported by Paschke et al. (Pasche et al., 2005) that the electrostatic potential of the waveguide surface has only a moderate influence on the secondary deposition and can be efficiently screened by the thin primary irreversible layer, whose properties govern the following deposition process. This can be justified by the fact that the extracts considered here contain a substantial amount of soluble ions so that the expected electrical double layer thickness is below 1 nm. Therefore electrostatic surface effects act only over a very short range, which is moreover further screened by the irreversible primary layer.

Deposition at elevated temperatures

Prior to the deposition measurements, the temperature response of the bare waveguide in pure water was investigated. The waveguide thickness t_F and refractive index n_F were evaluated (see Supplementary Information) with the n_C and n_S values reported in **Table 1**. As shown in **Figure 3**, an increase in the waveguide thickness and a decrease in refractive index were observed with increasing temperature. We note that the temperature response slightly varies between individual waveguides, although the general trend is always the same and relative changes in waveguide properties are very similar. As indicated by Saini et al. (Saini et al., 1994) the change in the waveguide thickness can be attributed to thermal dilatation of the waveguide material.

It is worth noting that in the temperature response experiments conducted in pure water, when the waveguide was cooled down to ambient temperature, the waveguide parameters were slightly different compared to those before heating. This may indicate a gradual hydrolysis and possibly dissolution of the silica coated waveguide, particularly at higher temperatures. Therefore we minimized the heat exposure of the waveguide in water to a minimum necessary time. On the other hand, changes of the waveguide optical parameters were not observed during the extract

deposition runs. The thin layer deposited from the extract can effectively protect the waveguide from hydrolysis and dissolution reactions in two ways. First, it can partially isolate the oxide surface from contact with the solution and secondly it reduces the mass transfer from the oxide surface to the bulk liquid. All the other parameters needed to estimate the deposited mass from are reported in **Table 1**.

In **Figure 4a** and **Figure 4b** we show a typical deposition experiment for the coffee extract at 60℃. All deposition runs started from a waveguide which had already undergone a primary deposition at ambient temperature, and therefore was covered by an irreversible primary layer. Accordingly, we refer to these experiments as secondary deposition runs in the following sections. The adopted experimental procedure is described in the experimental section and in the case of the experiment in **Figure 4** is reported in detail in **Table S1**. The last column in the table refers to the temperature which is shown in **Figure 4a**.

In **Figure 4b** the deposited mass is given as a function of time for silica coated waveguide for the different periods listed in **Table S1**. It is seen that as soon as the extract enters the measuring cell (period C) the deposited mass increases abruptly while at later times it follows an almost linear, relatively slow, increase which constitutes the secondary growth of the deposit. The first jump in deposited mass is due to the adsorption of the small electrolytes on the primary irreversible layer. This is a rather fast process and the deposition of large molecules in such a small time is probably negligible for the secondary deposition runs. In order to determine the deposited mass it is necessary to bring the surface of the waveguide after deposition at the desired temperature back to its initial state, i.e. in the presence of pure water at 25ºC. The total irreversibly deposited mass of the coffee extract is then computed as the difference between the mass measured at ambient temperature in water before the deposition (point M_1) and after water washing for one hour (point M_2). The corresponding average deposition rate is given as the increment of deposited mass divided by the exposure time at the elevated temperature.

It is worth noting that the average deposition rate determined by this method agrees well with the one obtained from the slope of the deposited mass curve as a function of time during period C in shown in **Figure 4b**. This is further supported by data collected for a moderately diluted extract over a range of temperatures shown in **Figure 5**. This confirms that the two ways of measuring the deposition rate, referred to as online and off-line respectively, yield comparable results. Therefore the thickness of the solid layer deposited on the waveguide after a certain duration of the deposition process corresponds to the secondary deposition rate measured during

period C. The electrolytes and other reversibly adsorbed species responsible for the sudden jump in the adsorbed mass at the very beginning of period C are all removed during the washing period E.

As can be seen from the semi logarithmic plot in **Figure 6**, the deposition rate of the original extract (solid circles) gradually increases by over two orders of magnitude when the temperature increases from 25 ℃ to 65 ℃, beyond which the deposition rate does not increase any further. The apparent plateau in the deposition rate above 65 ℃ was also confirmed by gravimetry measurements (see below) and it could be due to a diffusion limited regime for the transport from the bulk to the interface.

Effect of extract composition on deposition kinetics

The assembly of molecules and particles among themselves as well as at interfaces is controlled by their mutual interactions. Repulsive interactions, typically electrostatic or steric, between depositing entities are required in order to prevent mutual aggregation as well as surface fouling. Electrostatic interactions between colloidal particles are modulated most readily by solution pH and electrolyte concentration. Coffee extracts considered here contain molecules and colloidal particles with dissociable groups which are negatively charged at the normal extract pH values ~5, as indicated by electrophoretic mobility measurements of diluted extracts (zeta potential –15 mV).

In an attempt to control deposition kinetics through electrostatic interactions, we studied deposition by modifying pH to values 4.0 and 6.5 (from the natural pH of 5) at ambient temperature and at 65 ℃. As expected, by increasing pH the negative charges on the colloids increase, thus leading to slower deposition. In particular, the data reported in **Table 3** show that the increase of pH from 4 to 6.5 results in a decrease of the secondary deposition rate by a factor of 2. An even more pronounced decrease was observed at 65 ℃, with a reduction of the secondary deposition rate by a factor of 5 when increasing pH from 4 to 6.5.

The measured secondary deposition rates as a function of temperature are shown in **Figure 6** for extracts at various solid concentrations: the original extract at 13.3 wt% and those diluted with pure water to 1.3, 0.28, 0.14 and 0.034 wt%. We note that due to a strong buffering effect of the coffee extract, the pH values of the diluted extracts were close to that of the original extract (pH 5), with the highest value of pH 5.5 for the most diluted extract (0.034 wt%). From the data in the figure we observe that the rate of secondary deposition at the ambient temperature is only little sensitive to the extract concentration. Dilution of the original extract by a factor of up to 400

results in not more than a two fold decrease in the deposition rate, which at ambient temperature is only barely distinguishable from the experimental error. In particular, we see that the deposition rate for diluted extracts (solid concentration below 1.3 wt%) is largely independent of the extract concentration. This could be explained by recalling that there is always a reversibly deposited layer present at the surface in contact with the extract. Let us assume that this reversible layer is dense enough at all concentrations considered here so as to effectively saturate the underlying irreversibly bound layer. Then the rate of growth of the irreversible layer may be simply driven by incorporation of the loosely deposited material saturating the interface, and hence it would be essentially independent from the solution composition. However, this does not explain why the deposition rates at elevated temperatures from the original extract are much higher than from diluted ones.

In **Figure 7** we show the Arrhenius plot for deposition rates, where the data for the original (13.3 wt%) and the most diluted extract (0.036 wt%) are compared. The activation energy for deposition of the original extract was found to be about 130 kJ/mol, corresponding to an increase of the deposition rate by more than two orders of magnitude between 25 and 65℃. However, the deposition rate for the diluted extract, increased by less than 10 fold between 25 and 70℃ corresponding to an activation energy of about 30 kJ/mol. The difference in activation energies between the original and diluted extracts indicates that there is a different deposition mechanism operating in the two cases. In order to consider this in more detail, let us look first at aggregation in bulk coffee extracts upon their heating.

As fouling is primarily driven by interactions between depositing entities themselves rather than between depositing entities and the original surface, it is instructive to consider a possible relationship between surface deposition and aggregation in the bulk suspension. Here we used static light scattering to investigate the Brownian aggregation of colloidal particles in the bulk extracts at various dilutions and temperatures. In **Figure 8a** we show the measured scattered light intensity for the 200 times diluted extract after heating for 1 hour at the indicated temperatures. The pattern corresponds to gradual aggregation of smaller particles to larger clusters. There is a strong increase in the mean radius of gyration with increasing temperature, as can be seen in **Figure 9**. The observed behavior is very similar to the one found in **Figure 6** for the rate of deposition.

This is further supported by the fact that the activation energy for deposition from diluted extracts observed in **Figure 7** is of the same order of magnitude as for the so-called reaction

limited aggregation, where a typical energy barrier for aggregation is on the order of 10kT (Hunter, 2001), corresponding to the activation energy of 25 kJ/mol. These results indicate a correlation between irreversible aggregation in solution at elevated temperatures and secondary surface deposition in diluted coffee extracts.

A scattered intensity pattern very different from the one observed in diluted extracts was found when the original extract was heated at higher temperatures, as shown in **Figure 8b**. It appears that large particles of the order of tens of microns emerge after heating at elevated temperatures, although a good portion of the original colloidal particles is still present in the system. This indicates that in the original extract there is an irreversible formation of large aggregates upon heating, indicative of an association or a phase transition, as opposed to the gradual cluster-cluster aggregative growth seen in diluted extracts. These larger aggregates can then either directly assemble at the surface, or be deposited from the solution, in either case leading to much higher deposition rates compared to diluted extracts. These results suggest that the aggregation and deposition mechanisms in coffee extracts are strongly dependent on their concentration. It is worth noting that concentration driven association phenomena have been observed using light scattering in moderately concentrated solutions of peptides (Javid et al., 2011), proteins (Le Bon et al., 1999) and polysaccharides (Burchard, 2001), as well as in coffee extracts using viscosimetry (Redgwell et al., 2005).

Microscopy and gravimetric study

Scanning electron microscopy images of surfaces before and after deposition were taken in order to complement the information obtained by OWLS. Images of bare silica surface are flat and featureless down to resolution length scales of tens of nanometers, as shown in **Figure S1a**. The primary layers detected by OWLS are not visible by SEM and the corresponding image looks like those of the bare surface, even when a scratch to the primary layer is done. Missing contrast between the original surface and the deposited layer indicates information that the primary layer is uniform and homogeneous at the used resolution.

The secondary deposited layer on silica surface exposed to the extract at 50°C for 5 minutes can be made visible through SEM by scratching it to enhance the contrast between the layer and the surface (**Figure S1b**). The mass of the secondary deposit measured by OWLS for these conditions was about $1 mg.m^{-2}$ which was on the top of the primary layer constituted approximately by another 1 $mg.m^{-2}$. The contrast between surface and deposited layer was stronger in the case where the surface was exposed to the extract at 70°C for five minutes, as

shown in **Figure S1c**. In this case the mass measured by OWLS during the secondary deposition was 6 $mg.m^{-2}$, again on top of $1mg.m^{-2}$ of primary layer. Visual inspection of the SEM pictures indicates that in all cases the deposited layers were homogeneous and uniformly covering the exposed surfaces.

We further used gravimetry in order to measure the deposition rates at longer deposition times, and therefore for thicker deposited layers. As mentioned above, the gravimetry measurements can be performed only after an appreciable amount of mass has been deposited, which imposes a lower limit to the applicability of this method, which happens to be very close to the upper limit of OWLS. Therefore with this technique one can compare the deposition rates and deposited mass over longer time for dense, concentrated extracts and follow the history of the deposition process beyond the limits of OWLS. This also gives us the opportunity to verify the compatibility between these two techniques.

One important aspect in the design of these experiments is that in the measurement cells used for gravimetry and OWLS the hydrodynamic conditions at the deposition surface should be similar. As described in the experimental section this is obtained by a proper design of the gravimetric cell which in the experiments discussed in the following led to a velocity gradient at the surface equal to about $500s^{-1}$. Measurements were performed for the coffee extract at 65°C. The results in **Figure 10** show that the deposited mass as a function of time increases in a log-log plot in a consistent manner going from the short time OWLS measurements (diamonds) to the long-time gravimetric measurements (squares). This results in comparable deposition rates equal to about 1 $mg.m^{-2}.min^{-1}$, as determined by the two methods.

Gravimetric experiments have been performed using the original extract to measure the deposition rates at higher temperatures, i.e. 73 and 83°C.The obtained values are very similar to the one measured at 65°C, thus confirming the plateau in the deposition rate shown in **Figure 6** which was obtained by OWLS.

Conclusions

The deposition kinetics of an industrial coffee extract at wide range of temperatures was studied by OWLS and gravimetry. The first step in deposition formed a primary layer of about 1 $mg.m^{-2}$ on all the considered surfaces. At ambient temperature the secondary exposure of the primarily covered surface leads to reversible deposition, attributed to the electrolyte adsorption.

Temperature and concentration were found to be the main operating parameter driving deposition, which in the original extract reached a maximum rate at 65°C. Gravimetry was used as an independent method to measure the deposition rates. A comparison of the deposition rates, measured by gravimetry at longer times and by OWLS at shorter times, shows a very good consistency between the two methods. Deposition rates at ambient temperature were only little dependent on extract concentration, although they increase moderately with decreasing extract pH between 6.5 and 4. Activation energies for deposition kinetics were determined for both the original and diluted extracts. The activation energy for the original extract (solid concentration 13.3 wt%) was found to be about 130 kJ/mol between 25 and 65°C. However, the activation energy for diluted extracts was only about 30 kJ/mol. This can be due to the fact that the surface in contact with the diluted extracts is saturated with a loosely bound layer of material, which gradually becomes incorporated into irreversibly bound deposits. Therefore the buildup of the irreversibly bound deposit is independent of the extract concentration, provided that it is sufficient to reversibly saturate the available surface. In contrast, the original concentrated extract exhibits an irreversible association of suspended entities to large clusters at elevated temperatures, as indicated by static light scattering, leading to a different deposition mechanism with much higher deposition rates at higher temperatures. Our findings contribute to better understanding of mechanism and kinetics of deposition from protein/polysaccharide aqueous systems, which is a major cause of fouling at heat exchange surfaces of evaporators in production of instant coffee powders and other similar operations. In particular, the knowledge of deposition kinetics and corresponding activation energies will allow to determine time evolution of deposit thickness on evaporator walls and to assess its effect on heat transfer coefficients as a function of operating time and temperature. This will help to guide better design and improved operation of relevant processes in food and chemical processing industries.

Acknowledgements

This work was supported by Nestlé and by the Swiss Commission for Technological Innovation (KTI, Grant No. 5976.1). We would like to thank Dr. Remy Liardon and his colleagues from the Nestlé Product Technology Centre Orbe, Switzerland, for many fruitful discussions.

References

Anema, S. G. (2000). Effect of milk concentration on the irreversible thermal denaturation and disulfide aggregation of beta-lactoglobulin. Journal of Agricultural and Food Chemistry, 48, 4168-4175. DOI: 10.1021/jf991173e

Burchard, W. (2001). Structure formation by polysaccharides in concentrated solution. Biomacromolecules, 2, 342-353. DOI: 10.1021/bm0001291

Changani, S. D., BelmarBeiny, M. T. & Fryer, P. J. (1997). Engineering and chemical factors associated with fouling and cleaning in milk processing. Experimental Thermal and Fluid Science, 14, 392-406. DOI: 10.1016/S0894-1777(96)00141-0

Defeijter, J. A., Benjamins, J. & Veer, F. A. (1978). Ellipsometry as a Tool to Study Adsorption Behavior of Synthetic and Biopolymers at Air-Water-Interface. Biopolymers, 17, 1759-1772. DOI: 10.1002/bip.1978.360170711

Extrand, C. W. (1994). Spin-Coating of Very Thin Polymer-Films. Polymer Engineering and Science, 34, 390-394. DOI: 10.1002/pen.760340503

Grancic, P., Illeova, V., Polakovic, M., Sefcik, J. (2012). Thermally induced inactivation and aggregation of urease: experiments and population balance modelling. Chemical Engineering Science, 70, 14-21. DOI: 10.1016/j.ces.2011.07.050

Griesser, H. J., Hartley, P. G., McArthur, S. L., McLean, K. M., Meagher, L. & Thissen, H. (2002). Interfacial properties and protein resistance of nano-scale polysaccharide coatings. Smart Materials & Structures, 11, 652-661. DOI:10.1088/0964-1726/11/5/305

Haarmans, M. T. & Bedeaux, D. (1995). Optical Properties of Thin Films up to Second Order in the Thickness. Thin Solid Films, 258, 213-223. DOI: 10.1016/0040-6090(94)06395-8

Höök, F., Vörös, J., Rodahl, M., Kurrat, R., Böni, P., Ramsden, J. J., Textor, M., Spencer, N. D., Tengvall, P., Gold, J. & Kasemo, B. (2002). A comparative study of protein adsorption on titanium oxide surfaces using in situ ellipsometry, optical waveguide lightmode spectroscopy, and quartz crystal microbalance/dissipation. Colloids and Surfaces B: Biointerfaces, 24, 155–170 DOI:10.1016/S0927-7765(01)00236-3

Huang, N.-P. (2002). Biochemical Interactions of Surface-Bound PEG Copolymers. PhD Thesis, ETH, Zurich.

Hunter, R. J. (2001). Foundations of Colloid Science. Oxford University Press.

561 Javid, N., Vogtt, K., Roy, S., Hirst, A. R., Hoell, A., Hamley, I. W., Ulijn, R. V., Sefcik, J.
562 (2011). Supramolecular structures of enzyme clusters. Journal of Physical Chemistry Letters, 2,
563 1395–1399. DOI: 10.1021/jz200446j
564 Jong, P. (1997). Impact and Control of Fouling in Milk Processing. Trends in Food Science &
565 Technology, 8, 401-405. DOI: 10.1016/S0924-2244(97)01089-3
566 Kosmulski, M. (2001). Chemical properties of Material Surfaces. Dekker.
567 Kroslak, M., Sefcik, J. & Morbidelli, M. (2007). Effects of Temperature, pH and Salt
568 Concentration on β-Lactoglobulin Deposition Kinetics Studied by Optical Waveguide Lightmode
569 Spectroscopy. Biomacromolecules, 8, 963-970. DOI: 10.1021/bm060293+
570 Lavalle, P., Picart, C., Mutterer, J., Gergely, C., Reiss, H., Voegel, J. C., Senger, B. & Schaaf, P.
571 (2004). Modeling the buildup of polyelectrolyte multilayer films having exponential growth.
572 Journal of Physical Chemistry B, 108, 635-648. DOI: 10.1021/jp035740j
573 Le Bon, C., Nicolai, T. & Durand, D. (1999). Growth and structure of aggregates of heat-
574 denatured β-Lactoglobulin. International Journal of Food Science and Technology, 34, 451-465.
575 DOI: 10.1046/j.1365-2621.1999.00310.x
576 Mann, E. K. (2001). Evaluating optical techniques for determining film structure: Optical
577 invariants for anisotropic dielectric thin films. Langmuir, 17, 5872-5881. DOI:
578 10.1021/la001746d
579 Nakanishi, K., Sakiyama, T. & Imamura, K. (2001). On the adsorption of proteins on solid
580 surfaces, a common but very complicated phenomenon. Journal of Bioscience and
581 Bioengineering, 91, 233-244. DOI: 10.1016/S1389-1723(01)80127-4
582 Nellen, M. (1992). Integrated Optical Input Grating Couplers as Direct Chemo and Biosensors.
583 PhD Thesis, ETH, Zurich.
584 Pasche, S., Voros, J., Griesser, H. J., Spencer, N. D. & Textor, M. (2005). Effects of ionic
585 strength and surface charge on protein adsorption at PEGylated surfaces. Journal of Physical
586 Chemistry B, 109, 17545-17552. DOI: 10.1021/jp050431+
587 Picart, C., Ladam, G., Senger, B., Voegel, J. C., Schaaf, P.,& Gergely, C. (2001). Determination
588 of structural parameters characterizing thin films by optical methods: A comparison between
589 scanning angle reflectometry and optical waveguide lightmode spectroscopy. Journal of
590 Chemical Physics, 115, 1086-1094. DOI: 10.1063/1.1375156

591 Picart, C., Gergely, C., Arntz, Y., Voegel, J. C., Schaaf, P.,& Senger, B. (2004). Measurement of
592 film thickness up to several hundreds of nanometers using optical waveguide lightmode
593 spectroscopy. Biosensors & Bioelectronics, 20, 553-561. DOI: 10.1016/j.bios.2004.03.005
594 Redgwell, R. J., Schmitt, C., Beaulieu, M. & Curti, D. (2005). Hydrocolloids from coffee:
595 physicochemical and functional properties of an arabinogalactan-protein fraction from green
596 beans. Food Hydrocolloids, 19, 1005-1015. DOI: 10.1016/j.foodhyd.2004.12.010
597 Relkin, P. (1996). Thermal unfolding of β-lactoglobulin, α-lactalbumin, and bovine serum
598 albumin. A thermodynamic approach. Critical Reviews in Food Science and Nutrition, 36, 565-
599 601. DOI:10.1080/10408399609527740
600 Saini, S., Kurrat, R., Prenosil, J. E. & Ramsden, J. J. (1994). Temperature Dependence of
601 Pyrolyzed Sol-Gel Planar Waveguide Parameters. Journal of Physics D-Applied Physics, 27,
602 1134-1138. DOI:10.1088/0022-3727/27/6/009
603 Sava, N., Van der Plancken, I., Claeys, W. & Hendrickx, M. (2005). The kinetics of heat-induced
604 structural changes of β-lactoglobulin. Journal of Dairy Science, 88, 1646-1653. DOI:
605 10.3168/jds.S0022-0302(05)72836-8
606 Schubert, D. W. (1997). Spin coating as a method for polymer molecular weight determination.
607 Polymer Bulletin, 38, 177-184. DOI: 10.1007/s002890050035
608 Sefcik, J., Kroslak, M. & Morbidelli, M. (2002). Optical response of porous titania-silica
609 waveguides to surface charging in electrolyte filled pores. Helvetica Chimica Acta, 85, 3508-
610 3515. DOI: 10.1002/1522-2675(200210)85:10<3508::AID-HLCA3508>3.0.CO;2-M
611 Tiefenthaler, K. & Lukosz, W. (1989). Sensitivity of Grating Couplers as Integrated-Optical
612 Chemical Sensors. Journal of the Optical Society of America B-Optical Physics, 6, 209-220.
613 DOI: 10.1364/JOSAB.6.000209
614 Van Tassel, P. R. (2003). Statistical mechanical modeling of protein adsorption.
615 Materialwissenschaft Und Werkstofftechnik, 34, 1129-1132. DOI: 10.1002/mawe.200300703
616 Visser, J. & Jeurnink, T. J. M. (1997). Fouling of heat exchangers in the dairy industry.
617 Experimental Thermal and Fluid Science, 14, 407-424. DOI: 10.1016/S0894-1777(96)00142-2
618 Vogtt, K., Javid, N., Alvarez, E., Sefcik, J., Bellissent-Funel, M.-C. (2011). Tracing nucleation
619 pathways in protein aggregation by using small angle scattering methods. Soft Matter, 7, 3906-
620 3914. DOI: 10.1039/C0SM00978D

621 Voros, J. (2004). The density and refractive index of adsorbing protein layers. Biophysical
622 Journal, 87, 553-561. DOI: 10.1529/biophysj.103.030072
623

List of Tables

Table 1. Refractive indices as a function of temperature. T denotes temperature in ℃ and x_E is the weight concentration of solid content in coffee extract suspension (in g.cm^{-3}), $n_{C,E}$ denotes refractive index of coffee extract and n_{C,H_2O} denotes refractive index of water.

Parameter	25°C	T [°C]	Source
n_{C,H_2O}	1.331144	$n_{C,H_2O}^{25^oC} - \frac{75453.41\Delta T+2340.431\Delta T^2+6.363191\Delta T^3}{T.10^7+65.7081.10^7}$; where $\Delta T = T - 25$	a
$n_{C,E}$	$0.2090 x_E + n_{C,H_2O}^{25^oC}$	$(4.2725.10^{-6}T^2 - 4.665.10^{-4}T + 2.1795.10^{-1})x_E + n_{C,H_2O}^{T}$	measured by refractometer
n_S	1.525718	$1.52542 - 1.23.10^{-6}T$	*a*
a - reference (Saini et al., 1994)			

Table 2. Deposited amount of the irreversible primary layer from the coffee extract on various surfaces at ambient temperature.

Surface	Extract Solid Content [wt%]	Deposited Mass [$mg.m^{-2}$]
Silica	13.3	1.2
Silica	1.33	1.1
Silica	0.034	1.1
Niobia	13.3	1.2
Alumina	13.3	0.7
PEG-3.5-PLL	13.3	0.4
Polystyrene	13.3	0.90

Table 3. Influence of pH on secondary deposition rates of concentrated coffee extract.

Temperature [℃]	pH	Deposition Rate [$mg.m^{-2}.min^{-1}$]
25	4	0.006
	5	0.003
	6.5	0.003
65	4	1.6
	5	1.2
	6.5	0.3

List of Figures

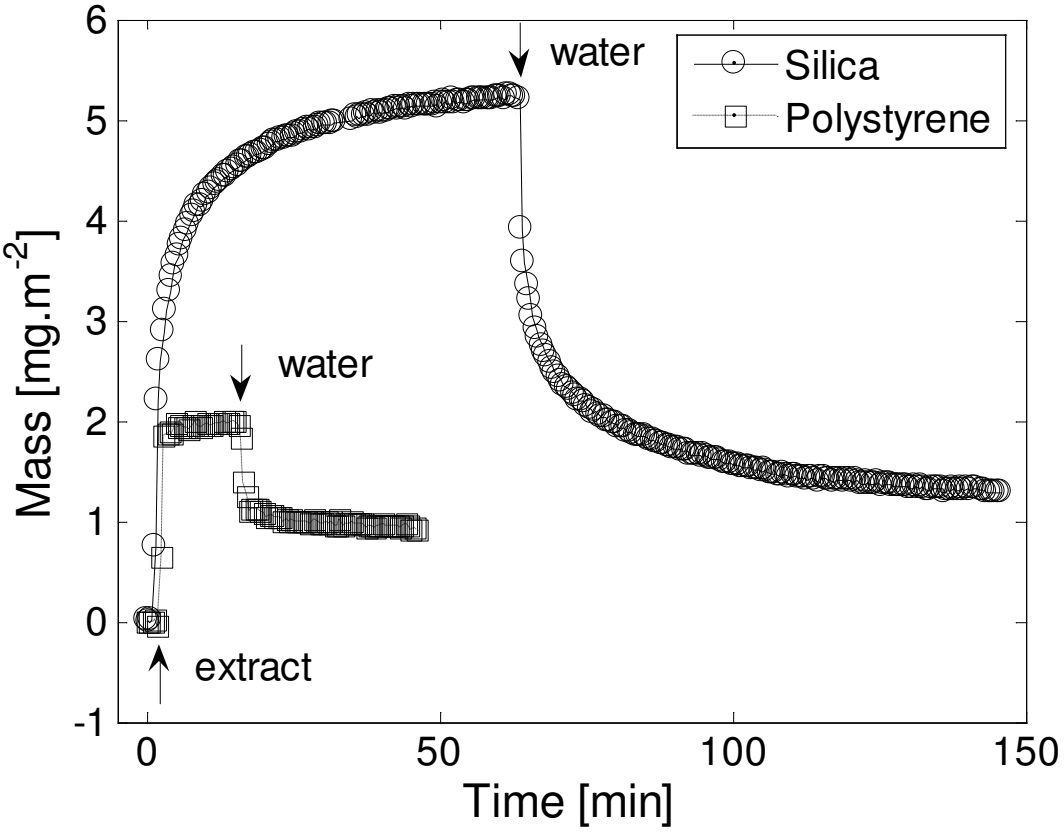

Figure 1. Primary exposure of silica and polystyrene surfaces to the original extract (13.3 wt%), pH 5.5 at 25ºC.

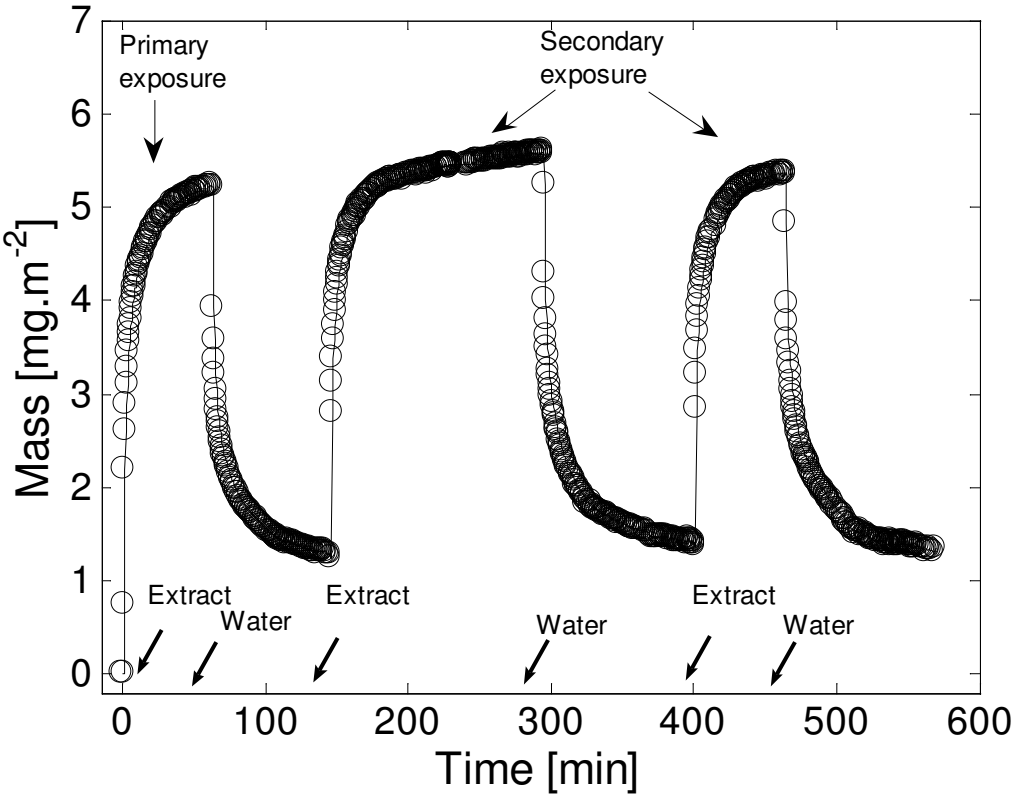

Figure 2. Three subsequent exposures of silica surface to the original extract at ambient temperature.

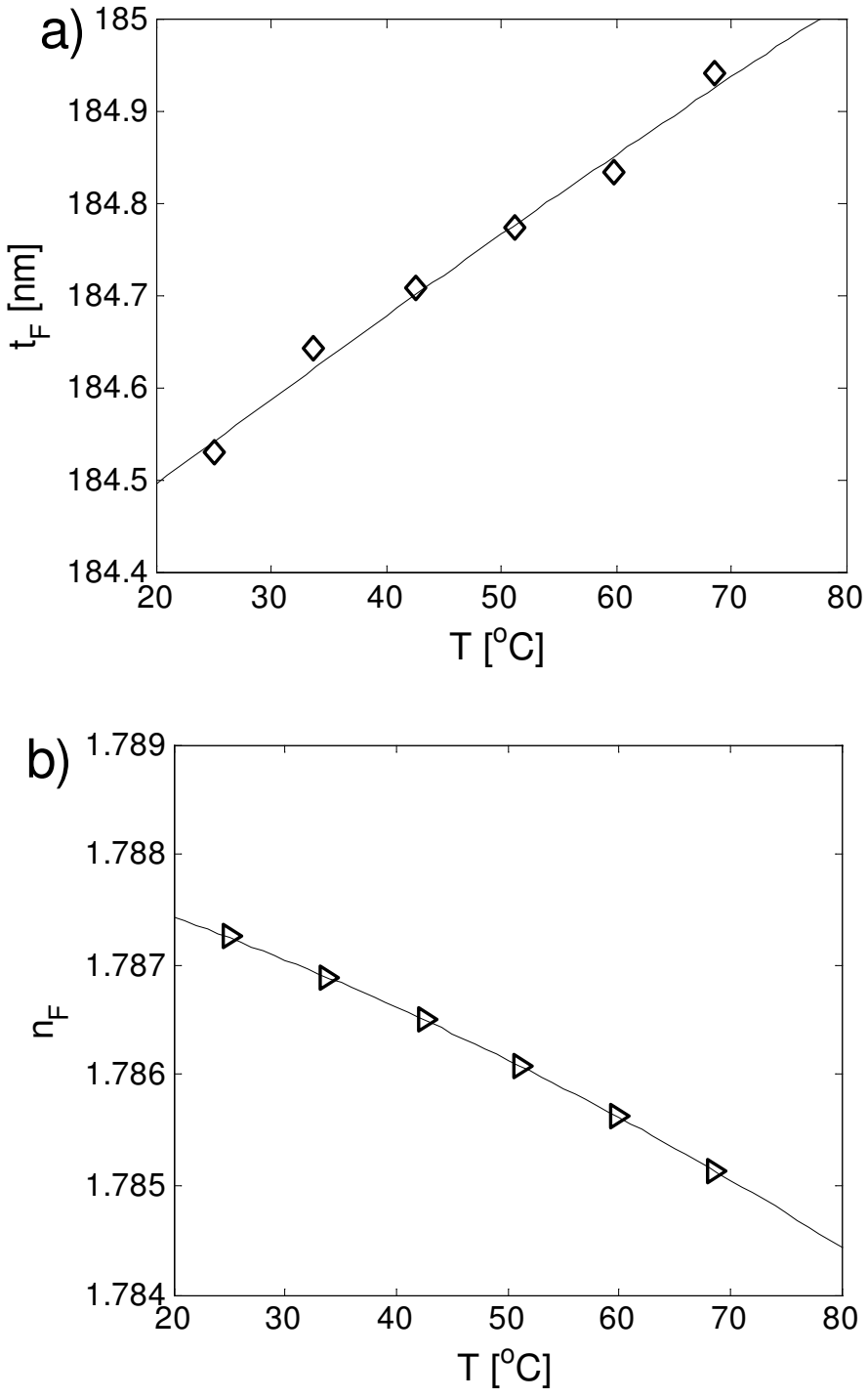

Figure 3. a) Waveguide thickness as a function of temperature. b) Waveguide refractive index as a function of temperature.

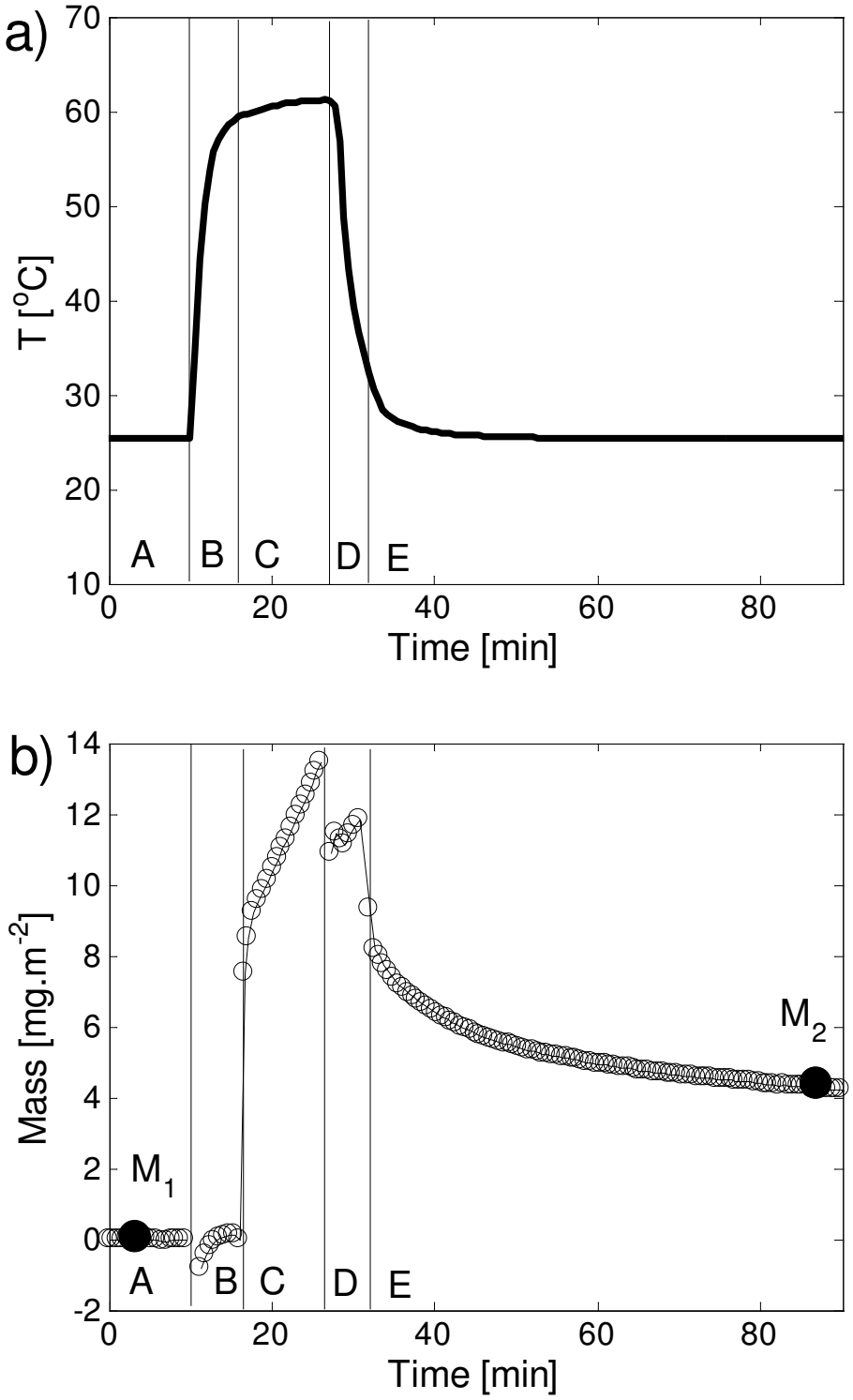

Figure 4. a) Cell temperature for secondary deposition experiment at 60℃. b) Deposited mass for secondary deposition experiment at 60℃.

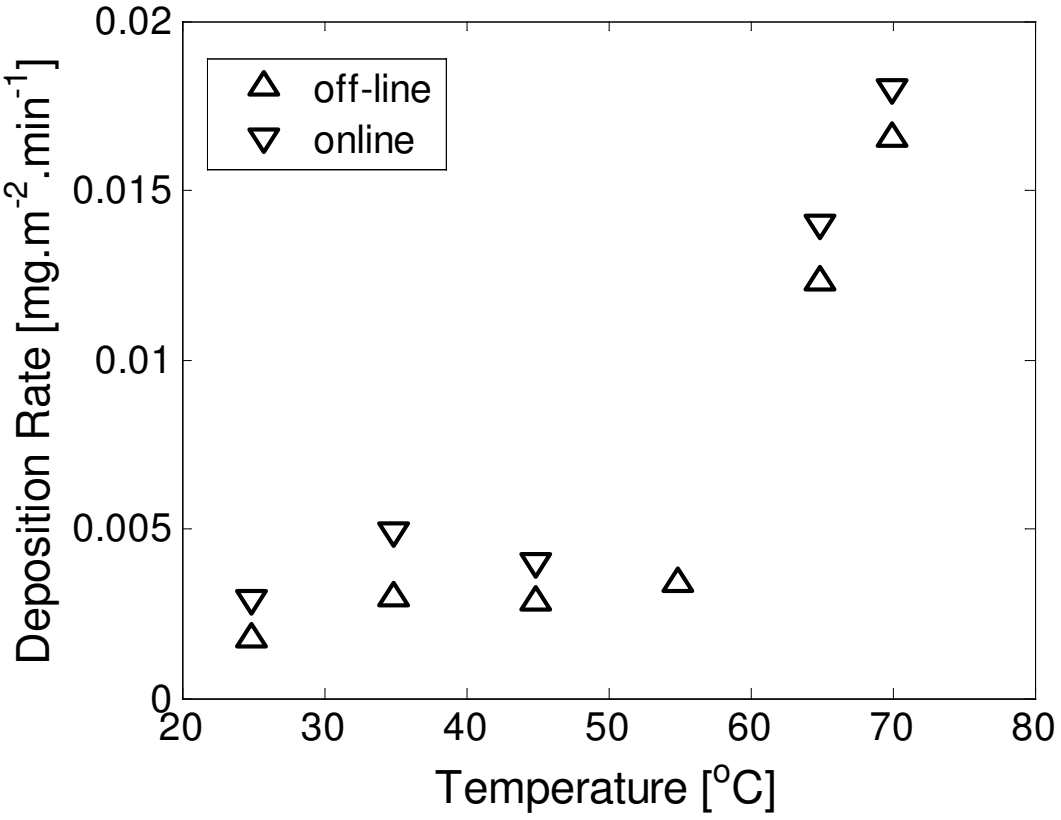

Figure 5. Comparison between deposition rates determined online and off-line for diluted extract (1.3 wt%) as a function of temperature.

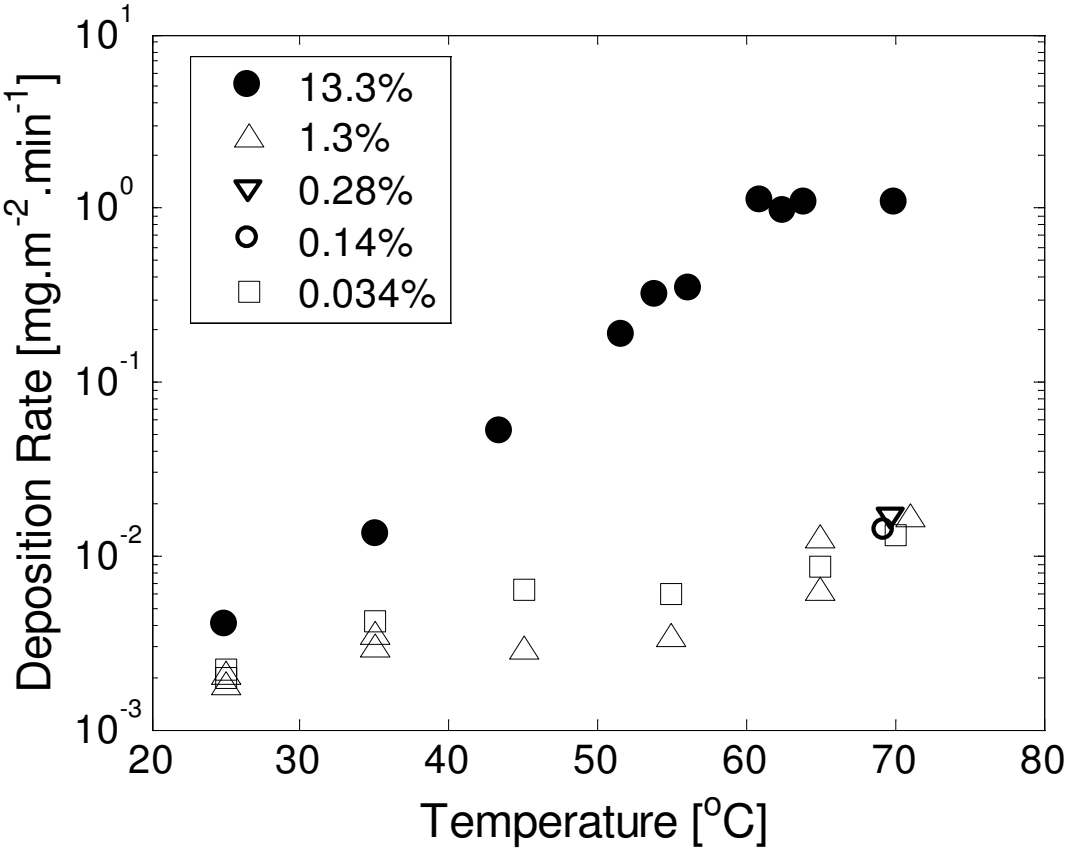

Figure 6. Deposition rates for the original extract as a function of temperature.

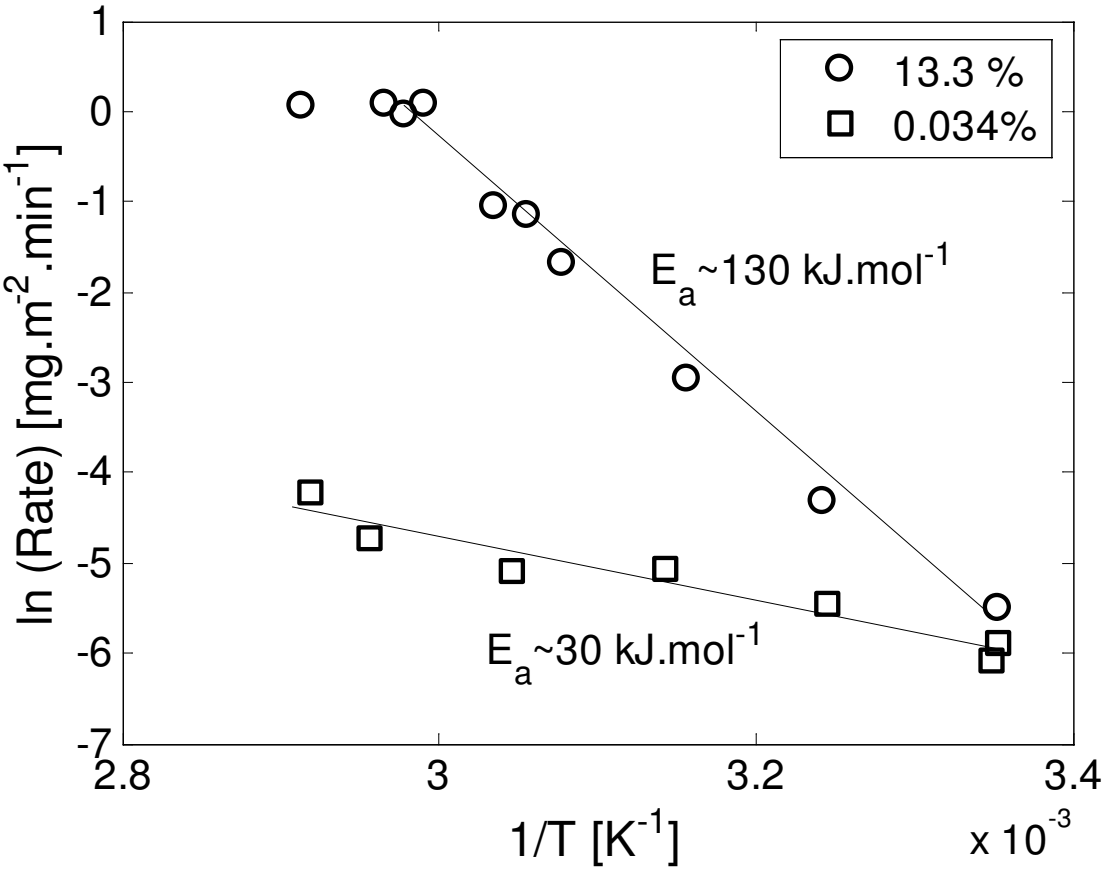

Figure 7. Arrhenius plot for the deposition rates.

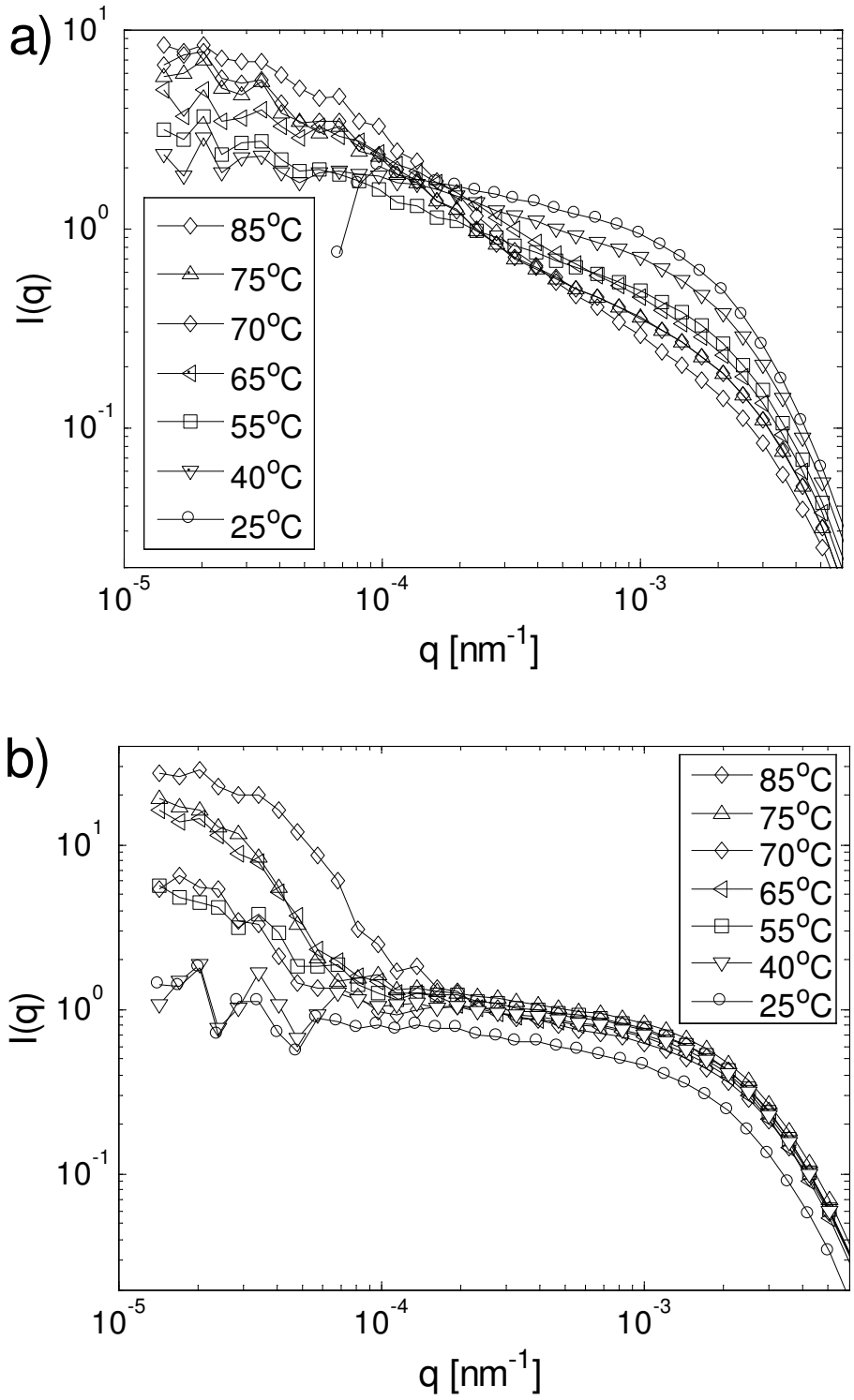

Figure 8. a) Scattered light intensity measured by SLS in 200 times diluted extract after aggregation at the indicated temperatures. b) Scattered light intensity measured by SLS in the original extract after aggregation at the indicated temperatures.

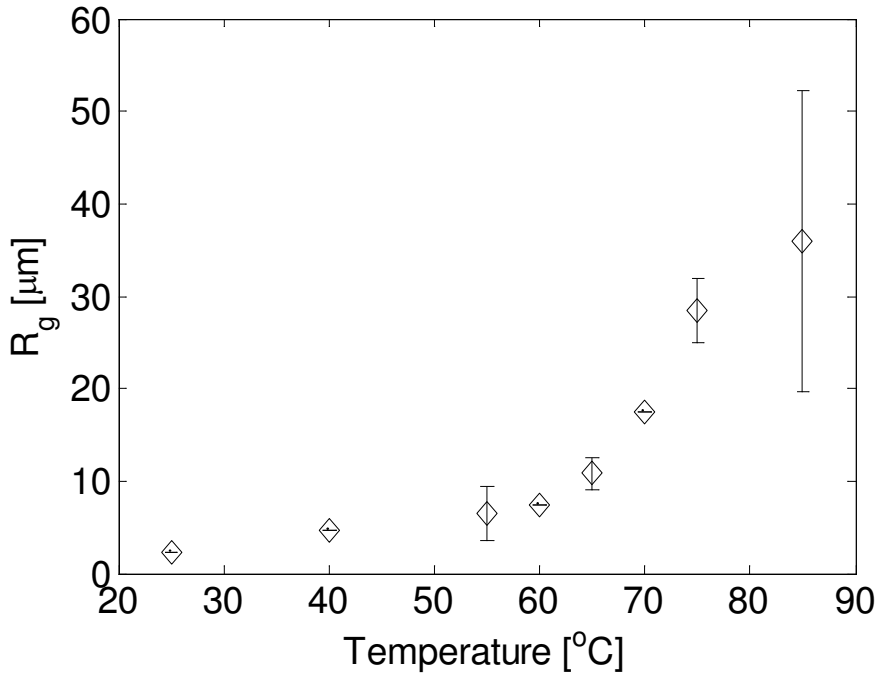

Figure 9. Radius of gyration measured by SLS for the 200 times diluted extract as a function of the aggregation temperatures. Error bars represent confidence intervals for radii of gyration estimated from data in Figure 8a.

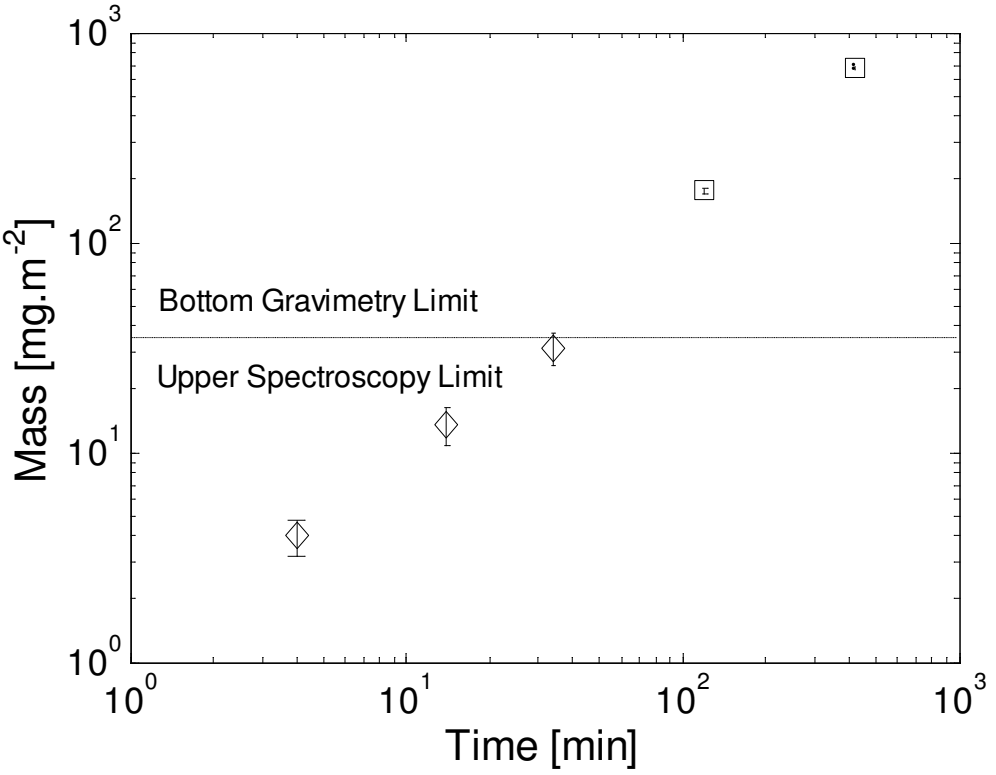

Figure 10. Deposited mass as a function of time at 65℃ for the original extract. Diamonds: OWLS; squares: gravimetry.